Shape of the coherent-population-trapping resonances and high-rank polarization moments

S. Gateva,* L. Petrov, E. Alipieva, and G. Todorov
Institute of Electronics, Bulgarian Academy of Sciences, 72 Tzarigradsko Chaussee, 1784 Sofia, Bulgaria

V. Domelunksen and V. Polischuk
SRI of Physics, University of St. Petersburg, 1, Ulyanovskaya, 198903, St. Petersburg, Russia
(Received 18 January 2007; revised manuscript received 15 March 2007; published 22 August 2007)

The shape of the coherent-population-trapping (CPT) resonances was investigated theoretically and experimentally at different laser powers. The CPT resonances were observed in fluorescence on the degenerate two-level system of the $(F_\varphi=2\rightarrow F_f=1)$ transition of the ^{87}Rb D_1 line by means of a Hanle effect configuration in an uncoated vacuum cell. Numerical simulations based on the density matrix formalism, which take into account the high-rank polarization moment (HRPMs) influence and the velocity distribution of the atoms, were used to calculate the shape of the nonlinear magnetic resonances. The comparison of the theoretical and experimental shapes of the CPT resonances demonstrated that the HRPMs influence the shape at all laser excitation powers, and this influence can be used to explain some peculiarities at the center of the CPT resonance shape.

DOI: 10.1103/PhysRevA.76.025401 PACS number(s): 32.80.Bx, 32.70.Jz, 32.10.Dk

There has been increasing interest in the investigation of the coherent-population-trapping (CPT) resonances, prepared and registered in different ways, because of many applications in high-resolution spectroscopy, magnetometry, lasing without inversion, laser cooling, ultraslow group velocity propagation of light, etc. [1–3]. In many applications to ensure a reliable operation, a good knowledge of the internal and external factors influencing the resonance shape is required [4].

The CPT resonance shape has been studied experimentally and theoretically in many works (see [1–6], and references therein). Most of the experimental investigations [1,2,7–11] were performed at low laser power, the shape of the resonances was practically Lorentzian, and the dependence of the resonance width on the laser power density was linear up to a few mW/cm^2. However, more precise investigations of the shape of the resonances showed that the theoretical shape could not reproduce the measured one [4,12–16], and in some works [4,12,14,16] theoretical dependences were proposed describing better the shape of the resonances for the particular experimental conditions.

At a high laser power, the influence of the multiphoton interactions increases. The coherences obtained, described in density matrix representation by the components $\rho_{MM'}$, are related in irreducible representation to the polarization moments ρ_q^k of rank k [$k=0,1,\ldots,2F_\rho$, $q=M-M'$, where F_ρ is the total angular momentum of the lower level]. For the case of $F_\rho=2$, the maximum rank of the polarization moment is $k=4$, the so-called hexadecapole moment.

The manifestation of the hexadecapole moments in laser-stimulated polarized fluorescence intensity was observed and described in terms of the iteration approach more than three decades ago [17]. Recently, the influence of the transverse components ($k=4$, $q=\pm 4$) of the Rb lower-level hexadecapole moments on the transverse ($k=2$, $q=\pm 2$) upper-level quadrupole components was discussed [18]. The influence of the high-rank polarization moments (HRPMs) on the nonlinear magneto-optical rotation resonances and their potential applications in nonlinear optics and in magnetometry were studied in [19]. Direct manifestation of the hexadecapole moment in the Hanle effect signals in some favorable conditions was observed in K_2 molecules [20].

In this work, theoretical investigation of the CPT resonance shapes registered in unpolarized fluorescence is performed taking into account the influence of the HRPMs. The results are compared with the CPT resonance shapes measured in fluorescence by means of the Hanle effect configuration. All investigations were carried out on the $(F_\varphi=2\rightarrow F_f=1)$ transition of the ^{87}Rb D_1 line (f denotes the excited level and φ the ground level), because this transition is almost nonoverlapping with any other.

The theoretical investigation of the HRPMs influence on the CPT signals was based on a well-known system of equations [17,21] for the density matrix tensor components ρ_q^k describing the interaction of the atomic system with a scanned magnetic field $\boldsymbol{B}_{scan}$, and a resonant, polarized laser field $\boldsymbol{E}$ (ω_0,t). According to [21] a decomposition of the density matrix in the (M,M') representation into tensor components $q=-k,\ldots,k$ is described as

$$\rho_q^k=(2F_\rho+1)^{1/2}\sum_{M,M'=-F_\rho}^{F_\rho}(-1)^{F_\rho-M}\begin{pmatrix}F_\rho & k & F_\rho\\ -M & q & M'\end{pmatrix}\rho_{MM'}. \tag{1}$$

The parentheses denote the Wigner $3j$ symbol.

Besides the clear physical meaning of the tensor components (ρ_0^0 describes the population; ρ_q^1, the orientation and ρ_q^2, the alignment of the atoms), this representation allows a diagonalization of the relaxation matrix - all relaxation parameters depend on the rank k of the components only.

In our recent works [7,22], the basic system [17,21] was modified to describe the interaction with an additional, ran-

*FAX: +359 2 9753201. sgateva@ie.bas.bg

domly oriented, field $\boldsymbol{B}'$ and concretized for the $F_\varphi=2\rightarrow F_f=1$ ^{87}Rb D_1 line transition and for the experimental geometry used. The quantization axis was chosen parallel to the electric vector $\boldsymbol{E}$ ($\equiv E_z$) of the laser field and the scanned magnetic field $\boldsymbol{B}_{scan}$ ($\equiv B_x$) was perpendicular to this axis.

Using the rotating wave approximation and assuming a single-frequency laser field, the system of equations was reduced to an algebraic one. Exact numerical solutions of the algebraic system were obtained for the following set of parameters: Rabi frequency ($\Omega_R=dE/h$); spontaneous emission transfer coefficients $\Gamma_{f\varphi}(k)$ and stray field $\boldsymbol{B}'$. All these parameters and the magnetic fields are given in units of the upper-level population decay rate $\gamma_f(0)$. The initial (without laser field broadening) low-level population relaxation rate constant $\gamma_\varphi(0)$ was determined by the time of flight for the atoms [$\gamma_\varphi(0)\approx 0.001\gamma_f(0)$]. We also assumed all rate constants $\gamma_\rho(k)$ for the tensor components ρ_q^k to be equal. The very recent experiments [19] give for the ratio $\gamma_\rho(2)/\gamma_\varphi(4)$ a value in the interval 0.7–0.9 for different powers of excitation. In the model used the transverse alignment of the upper level is neglected. This is why in the presentation below the indices k in the designation of the decay constants $\gamma_\rho(k)$ will be omitted.

The Maxwell velocity distribution of the atoms was taken into account. The solution for a given component ρ_q^k was obtained by summarizing the partial solutions for the subensemble of atoms with velocities in a given interval. The integration step was varied and the integration region was chosen to exceed $40\gamma_f$.

In the dipole approximation, the spontaneous emission intensity and absorption are defined only by the tensor components ρ_q^k with rank $k\leq 2$. The unpolarized fluorescence intensity $I_{f\varphi}^{unpol}$ can be written as [17,23]

$$I_{f\varphi}^{unpol}=C_0\left(\frac{f_0^0}{\sqrt{2F_f+1}}+(-1)^{F_f+F_\varphi+1}\sqrt{30}\times\begin{Bmatrix}1 & 1 & 2\\ F_f & F_f & F_\varphi\end{Bmatrix}f_0^2\right). \quad (2)$$

Only the two tensor components for the upper level, f_0^0 and f_0^2, describe the signal observed in this case. In linear approximation neither component depends on the magnetic field. The magnetic field dependence is the result of the transfer of coherence created on the low level, and it is a typical nonlinear effect. In a strong laser field, both these components will be influenced by the hexadecapole components of the ground state. This is why in our numerical modeling we focused our attention on the f_0^0 and f_0^2 tensor components, as well as on the high-rank optical coherences (octupole, $k=3$) and on the hexadecapoles ($k=4$) related to the ground state. The main part of the unpolarized intensity is determined by the upper-level population f_0^0.

Figure 1 presents the shapes of the CPT resonances calculated at different Rabi frequencies. For convenience in the comparison of the experimental and theoretical shapes, the magnetic field scan is also given in units of γ_f—the width of the upper level (~6 MHz). The split between the adjacent Zeeman sublevels of the ground state is 0.7 kHz/mG [1].

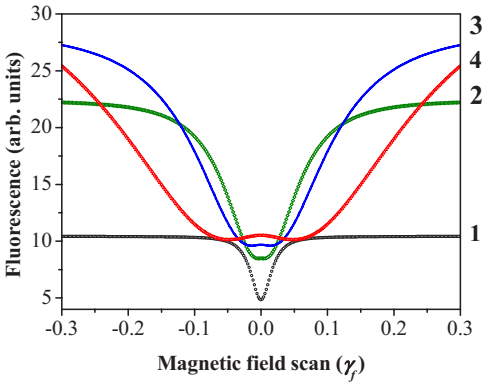

FIG. 1. (Color online) Calculated shape of the CPT resonances at different Rabi frequencies Ω_R: curve 1, $\Omega_R=\gamma_f$; curve 2, $\Omega_R=3\gamma_f$; curve 3, $\Omega_R=5\gamma_f$; curve 4, $\Omega_R=10\gamma_f$.

At relatively low power (Fig. 1, curve 1) the shape is close to Lorentzian; as the power is increased, the resonance broadens, and flattens at the center and an inverse narrow structure appears there (Fig. 1, curves 2–4). An evaluation of the effective (including field broadening) profiles widths γ_φ^{eff} gives values from $0.03\gamma_f$ to $0.2\gamma_f$.

The numerical simulation of our equations allows us to conclude that the main part of this inversion is due to conversion of the lower-level hexadecapole components φ_q^4 to the upper level observables. As the octupoles ρ_q^3 take part directly in the equations for the quadrupoles ρ_q^2, their influence on the shape and amplitude of the f_0^2 is essential.

In the case of power densities corresponding to Rabi frequencies of the order of 1 MHz ($\sim 0.2\gamma_f$), the calculated CPT resonance shape could not be visually distinguished from a Lorentzian, but in the difference between the calculated profile and its Lorentzian fit there was a specific structure at the center (Fig. 2). This structure is similar in shape to the one reported earlier in [13–15].

Measurements of the CPT resonance shapes were performed to check the shapes obtained theoretically. The experimental setup for measurement of the CPT resonances at different laser powers was the same as the one used in our previous investigations (Fig. 3) [5,24]. The CPT resonances were examined at room temperature (20 °C) in an uncoated

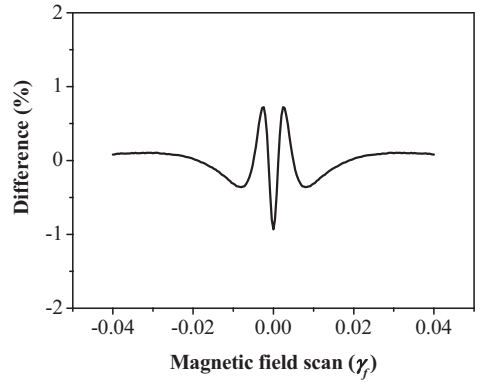

FIG. 2. Difference between calculated resonance shape and its Lorentzian profile fit at $\Omega_R=1$ MHz ($\sim 0.2\gamma_f$).

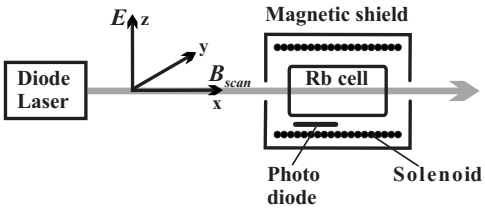

FIG. 3. Experimental setup geometry.

vacuum cell containing a natural mixture of Rb isotopes. A magnetic field, created by a solenoid, was applied collinearly to the laser beam. The fluorescence signals, detected by a photodiode placed close to the front window of the cell, were amplified and stored in a PC, which also controlled the magnetic field scan. As the CPT resonance amplitudes and widths are very sensitive to stray magnetic fields [7,24], the gas cell and the solenoid were placed in a three-layer μ-metal magnetic shield.

At relatively low power density of 1.7 mW/cm^2 (for a laser linewidth 50 MHz, corresponding to reduced Rabi frequency Ω_R=1 MHz), the measured CPT resonance shape was close to Lorentzian. The difference between the experimental profile and its Lorentzian fit is presented in Fig. 4. The shape and amplitude of this structure are similar to those reported in [13–15] and to the theoretical one (Fig. 2).

The comparison of the experimental and theoretical shapes at higher excitation powers is more complicated. Even at laser power density 1 W/cm^2 (corresponding to a reduced Rabi frequency Ω_R=25 MHz) (Fig. 5, curve 1) no dip or flattening as predicted by the theory (Fig. 1) was observed. Our previous investigations [5,24] have shown that the experimental CPT resonance has a complex shape—a narrow structure superimposed on a broader one. Both components have the same signs but different dependence on the laser power density and at high power density the amplitude and width of the resonances are strongly influenced by the narrow structure. There are different hypotheses about the origin of the narrow component, but they are not included in our theoretical model presented here. We tried to observe the influence of the HRPMs on the wide component shape, eliminating the narrow structure by applying an additional transverse magnetic field B_y. As was measured in [24], the

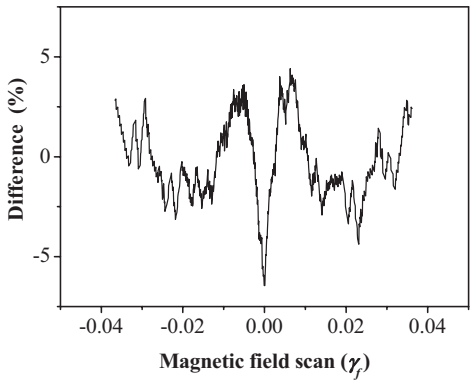

FIG. 4. Difference between the experimental resonance and its Lorentzian fit at Ω_R=1 MHz.

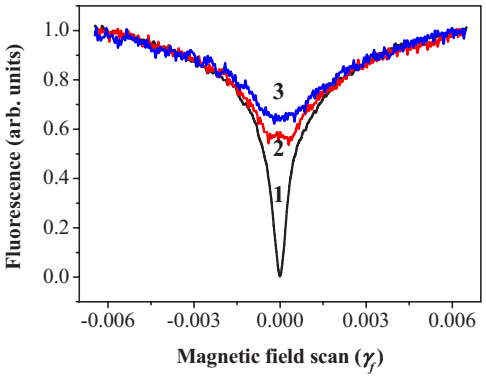

FIG. 5. (Color online) CPT signals measured around the center of the resonance at different magnetic fields B_y transverse to the polarization vector and to the propagation direction: curve 1, B_y=0 mG; curve 2, B_y=32 mG; curve 3, B_y=72 mG.

narrow structure is very sensitive to magnetic fields perpendicular to the polarization vector $\boldsymbol{E}$ ($\equiv E_z$) and $\boldsymbol{B}_{scan}$ ($\equiv B_x$). Magnetic fields B_y of the order of 10 mG destroy it, while the broader structure (which is ~150 mG in width) is practically not affected. The comparison of the central regions of the resonances observed at B_y=0 (Fig. 5, curve 1) and at B_y=32 mG (Fig. 5, curve 2) shows that at this power density the amplitude of the CPT resonance in a magnetic field is reduced twice and an additional inverted structure (about 5% in amplitude) appears. At higher magnetic fields, this inverted structure disappears (Fig. 5, curve 3).

Figure 6 presents the shapes of the CPT resonances calculated at different transverse magnetic fields B_y at a laser power corresponding to the Rabi frequency $\Omega_R=3\gamma_f$. At B_y=0 there is an inverted structure at the center of the resonance (Fig. 6, curve 1), which decreases in amplitude with increasing B_y (Fig. 6, curves 2 and 3) and disappears when the Larmor frequency $\mu_B g_F B_y/\hbar$ exceeds the width of this structure. A further increase of B_y causes a decrease of the amplitude of the whole resonance (Fig. 6, curve 4). As our theoretical model does not include the narrow structure of the resonance, the theoretical and experimental shapes can be

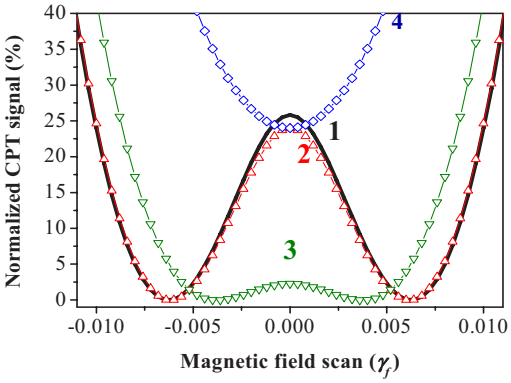

FIG. 6. (Color online) Fragment of the normalized calculated shape of the CPT resonances at different transverse magnetic fields B_y: curve 1, $B_y=0\gamma_f$; curve 2, $B_y=0.001\gamma_f$; curve 3, $B_y=0.005\gamma_f$; curve 4, $B_y=0.01\gamma_f$; $\Omega_R=3\gamma_f$; $\gamma_\varphi=0.0002\gamma_f$.

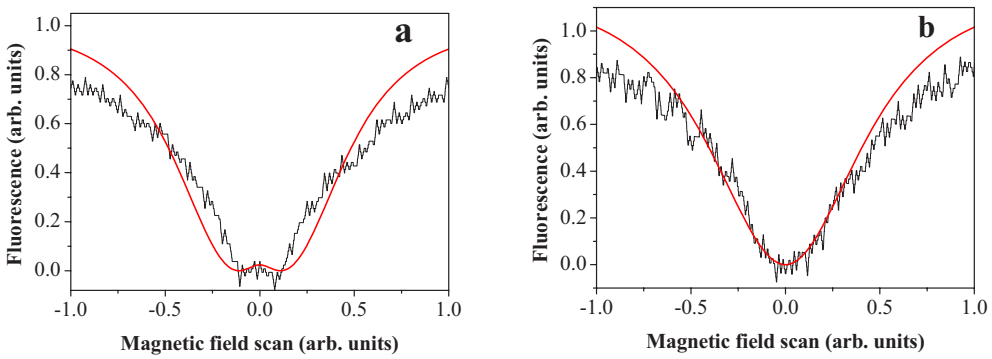

FIG. 7. (Color online) Comparison of the theoretical and experimental CPT resonance shapes at the center of the resonance at transverse magnetic field: (a) $B_y=0.001\gamma_f$ and (b) $B_y=0.01\gamma_f$.

compared only at magnetic fields B_y when the narrow structure is destroyed. The comparison of Fig. 5 (curves 2 and 3) and Fig. 6 (curves 3 and 4) shows that the theoretical shape changes repeat in general the shape changes of the experimental profiles.

The main difference between the calculated (Fig. 6) and the experimental (Fig. 5) resonance profiles in a strong laser field is the width of the resonances. As stated above, the coherent narrowing of the CPT resonances at high powers observed in our experiments [5] is not described by the model discussed here. Nevertheless, it is possible to compare the calculated and experimental shapes near the center of the resonances in B_y magnetic field. To compare them, the theoretical and the experimental curves were normalized to their Lorentzian fit. The results for two values of B_y are illustrated in Figs. 7(a) and 7(b) and a good agreement at the center of the resonance is demonstrated.

In conclusion, the comparative investigation performed of the shapes of the CPT resonances registered in unpolarized fluorescence shows that the HRPMs influence them at low excitation power and at high excitation powers as well. The HRPMs conversion is proved to cause the CPT resonance shape peculiarities at the center of the resonance: at low excitation power, a specific difference from the Lorentzian shape is observed, while at a high power of excitation, an inverted structure is registered. The results of this investigation are interesting for high-resolution spectroscopy, magnetometry, and metrology applications.

The authors are pleased to acknowledge stimulating discussions with M. Auzinsh, A. Gordon, L. Moi, and A. Weis and the financial support of the European Community (Project No. G6RD-CT-2001-00642) and the National Science Fund of Republic of Bulgaria (Grant No. F-1409/04).

[1] E. Arimondo, in *Progress in Optics*, edited by E. Wolf (Elsevier, Amsterdam, 1996), Vol. 35, p. 257.
[2] R. Wynands and A. Nagel, Appl. Phys. B: Lasers Opt. **68**, 1 (1999).
[3] D. Budker *et al.*, Rev. Mod. Phys. **74**, 1153 (2002).
[4] S. Knappe *et al.*, J. Opt. Soc. Am. B **18**, 1545 (2001).
[5] S. Gateva, E. Alipieva, and E. Taskova, Phys. Rev. A **72**, 025805 (2005).
[6] J. Vanier, Appl. Phys. B: Lasers Opt. **81**, 421 (2005).
[7] A. Huss *et al.*, J. Opt. Soc. Am. B **23**, 1729 (2006).
[8] J. Vanier, A. Godone, and F. Levi, Phys. Rev. A **58**, 2345 (1998).
[9] M. Erhard and H. Helm, Phys. Rev. A **63**, 043813 (2001).
[10] M. D. Lukin *et al.*, Phys. Rev. Lett. **79**, 2959 (1997).
[11] V. A. Sautenkov, M. M. Kash, V. L. Velichansky, and G. R. Welch, Laser Phys. **9**, 1 (1999).
[12] J. E. Thomas and W. W. Quivers, Jr., Phys. Rev. A **22**, 2115 (1980).
[13] E. Pfleghaar, J. Wurster, S. I. Kanorsky, and A. Weis, Opt. Commun. **99**, 3003 (1993).
[14] A. V. Taichenachev *et al.*, Phys. Rev. A **69**, 024501 (2004).
[15] S. Gateva, E. Alipieva, and E. Taskova, in Proceedings of the Fourth International Symposium on Laser Technologies and lasers, Plovdiv, Bulgaria, 2005, edited by N. Sabotinov, M. Nenchev, and V. Ribarov (April 2006), p. 299.
[16] F. Levi *et al.*, Eur. Phys. J. D **12**, 53 (2000).
[17] M. Ducloy, Phys. Rev. A **8**, 1844 (1973); **9**, 1319 (1974); B. Decomps, M. Dumont, and M. Ducloy, in *Laser Spectroscopy of Atoms and Molecules*, edited by H. Walther (Springer-Verlag, Berlin, 1976).
[18] A. I. Okunevich, Opt. Spectrosc. **91**, 177 (2001).
[19] S. Pustelny *et al.*, Phys. Rev. A **73**, 023817 (2006); V. V. Yashchuk *et al.*, Phys. Rev. Lett. **90**, 253001 (2005).
[20] M. Auzinsh and R. Ferber, *Optical Polarization of Molecules* (Cambridge University Press, New York, 2005).
[21] M. I. D'yakonov and V. I. Perel, Opt. Spectrosc. **20**, 101 (1966).
[22] G. Todorov *et al.*, Proc. SPIE **5449**, 380 (2004); V. Polischuk *et al.*, *ibid.* **6257**, 62570A (2006); D. Slavov *et al.*, in Proceedings of the Fourth International Symposium on Laser Technologies and lasers, Plovdiv, Bulgaria, 2005, edited by N. Sabotinov, M. Nenchev, and V. Ribarov (April 2006), p. 166.
[23] E. B. Alexandrov, M. P. Chaika, and G. I. Hvostenko, *Interference of Atomic States* (Springer-Verlag, Berlin, 1991).
[24] E. Alipieva, S. Gateva, E. Taskova, and S. Cartaleva, Opt. Lett. **28**, 1817 (2003).